

Uncooled 100-GBaud Operation of Directly Modulated Membrane Lasers on High-Thermal-Conductivity SiC Substrate

Suguru Yamaoka⁽¹⁾, Nikolaos-Panteleimon Diamantopoulos⁽¹⁾, Hidetaka Nishi⁽¹⁾, Takuro Fujii⁽¹⁾,
Koji Takeda⁽¹⁾, Tatsuhiro Hiraki⁽¹⁾, Shigeru Kanazawa⁽²⁾, Takaaki Kakitsuka⁽¹⁾, Shinji Matsuo⁽¹⁾

⁽¹⁾ NTT Device Technology Labs, NTT Corporation, 3-1 Morinosato Wakamiya, Atsugi-shi, Kanagawa, 243-0198 Japan, suguru.yamaoka.hm@hco.ntt.co.jp

⁽²⁾ NTT Device Innovation Center, NTT Corporation, 3-1 Morinosato Wakamiya, Atsugi-shi, Kanagawa, 243-0198 Japan

Abstract We have developed directly modulated membrane lasers on a high-thermal-conductivity SiC substrate, which exhibit bandwidth of >110 GHz at 25°C, and 74 GHz at 85°C by large relaxation oscillation frequency and optical feedback effect. We demonstrate 2-km transmission of 100-Gbit/s NRZ signals with uncooled operation. ©2022 The Authors

Introduction

Ever-increasing Internet traffic due to the constant development of Internet services has led to the need for standardizing 800-Gbit/s and 1.6-Tbit/s Ethernet [1]. At the same time, the operation of optical transmitters at a symbol rate of 100 GBaud is crucial in order to increase the data rate per lane. Currently, directly modulated lasers (DMLs) with uncooled operation are widely utilized as low-power-consumption and cost-effective transmitters in data center networks. Therefore, uncooled DMLs with 100-GBaud modulations are strongly desired. However, the 3-dB bandwidth f_{3dB} of DML is mainly limited by the relaxation oscillation frequency f_r (typically ~20 GHz at 25°C). In addition, since f_r is proportional to the square root of the bias current above the threshold [2], high-speed DMLs face the problem of increased power consumption. One way to overcome these issues is the utilization of optical feedback effects such as the detuned-loading effect and photon-photon resonance (PPR) [3-6]. Matsui et al. expanded the f_{3dB} of the 1.3- μ m distributed feedback (DFB) laser to 75 GHz by using these effects at 25°C [5]. However, the bandwidth at 50 (75) °C was 57 (33) GHz, which is insufficient for 100-GBaud modulation at high temperatures.

We previously proposed membrane lasers on SiC substrate in which thin III-V layers (typically 340 nm) are sandwiched by low-refractive-index SiC and SiO₂ layers [4]. Therefore, the optical confinement factor Γ is three times higher than that of the standard DMLs, which improves the modulation efficiency. The temperature increase in the active region can be suppressed when the bias current is increased thanks to the high thermal conductivity of SiC, and we were able to achieve a f_r of 42 GHz and a f_{3dB} of 60 GHz at 25°C. Furthermore, in the device with optical feedback,

PPR was observed at 95 GHz, resulting in a f_{3dB} of 108 GHz at 25°C and 256-Gbit/s four-level pulse amplitude modulation transmission. The next challenge is high-speed operation with uncooled operation. The f_r decreases when the operation temperature increases [7], which makes it difficult to achieve a flat frequency response with small-signal modulation. Moreover, while SiC provides good heat dissipation, the temperature of the active layer itself increases because the environmental temperature itself is rising. Thus, there are concerns about the degradation of the active layer due to heterogeneous integration on SiC.

In this work, we fabricated membrane lasers on SiC substrate and investigated the lasing properties at temperatures ranging from 25 to 85°C. Thanks to the PPR effect, we achieved a maximum f_{3dB} of >110 GHz at 25°C, 97 GHz at 55°C, and 74 GHz at 85°C. We also demonstrated the 2-km transmission of 100-Gbit/s (non-return-to-zero) NRZ signals at 25 and 85°C. This is the first demonstration of 100-GBaud operation at 85°C for any DML.

Device structure and design

Figure 1 shows a schematic diagram of the distributed reflector (DR) laser we fabricated consisting of three sections: (1) a 50- μ m-long

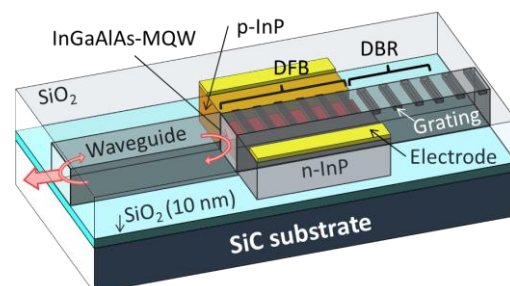


Fig. 1: Schematic diagram of the membrane laser on SiC substrate.

DFB section with a uniform grating, (2) a 60- μm -long distributed Bragg reflector (DBR) mirror, and (3) a 135- μm -long passive waveguide. We applied a low-damage O_2 -plasma-assisted direct bonding method to the InP and SiC substrates to fabricate the III-V membrane laser structure on the SiC substrate (see [4] for details of the fabrication process). Figure 2 shows a cross-sectional transmission electron microscope (TEM) image of the DFB section. A 5-nm-thick SiO_2 was deposited on both the InP and SiC substrates; the total thickness of the bonding SiO_2 layer was 10 nm. The active region was composed of a nine-period InGaAlAs multiple-quantum well (MQW), which was buried in the InP membrane layer with a thickness of ~ 340 nm. The lateral p-i-n structure enabled the lateral current injection into the MQWs.

As shown in Fig. 1, the reflection at the waveguide facet causes Fabry-Pérot (FP) interference between the facet and the front of the DFB section. The PPR effect occurs due to the interaction between the lasing mode and one of the FP modes, which enhances the EO response at the frequency difference of two of the modes. The FSR was set to 270 GHz.

Results and discussion

Figure 3(a) shows the output light versus bias current (L-I curve) at 25, 55, and 85°C. The stage temperature was controlled by a thermoelectric cooler, and the optical power was detected using a lensed fiber. The threshold currents at 25, 55, and 85°C were 2.9, 4.4, and 6.7 mA, respectively. A kink was observed at each temperature, and the PPR was observed at the current range before the kink. The maximum optical power coupled to the standard single-mode fiber (SSMF) at 25, 55, and 85°C was 0.82, 0.51, and 0.31 mW, respectively.

Figure 3(b) shows the lasing spectra at 25, 55, and 85°C, where the bias current was 7 mA. As can be seen, the rear DBR successfully selected the longer side mode of the DFB stopband. We also observed FP modes caused by the optical feedback from the waveguide facet acting as the PPR mode. When the current increases and then the temperature of the DFB section increases, the lasing mode is red-shifted. In contrast, the temperature of the DBR section remains constant. Thus, the frequency detuning between a lasing mode and a nearest-neighbour FP mode is changed, and mode hopping is observed when the detuning becomes small.

Next, we evaluated the dynamical modulation properties of the laser. Figures 4(a), (b), and (c) show the small-signal S_{21} responses at 25, 55, and 85°C, respectively. A light

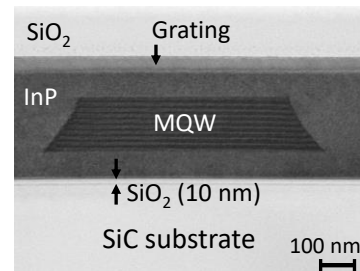


Fig. 2: Cross-sectional TEM image of DFB section.

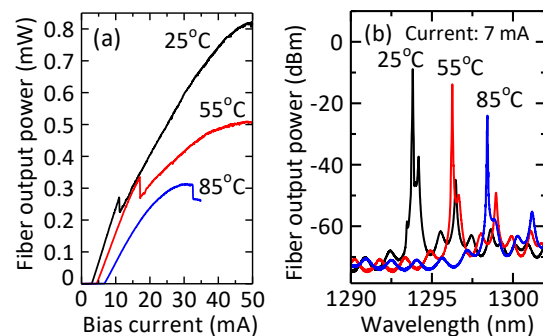


Fig. 3: (a) L-I curves at 25, 55, and 85°C. (b) Lasing spectra at 25, 55, and 85°C. The bias current was 7 mA.

component analyser (Keysight N4372E) able to operate at up to 110 GHz was used for these measurements. At 25 and 55°C, two PPR-occurrence regions were observed at two bias current regions. At 85°C, only the first PPR occurrence region was observed, since the current range of the second one was over the current at the thermal rollover. We were able to obtain a $f_{3\text{dB}}$ of 66 GHz at 9 mA and >110 GHz at 45 mA at 25°C, 70 GHz at 14 mA and 97 GHz at 50 mA at 55°C, and 74 GHz at 26 mA at 85°C. Relatively flat frequency responses were obtained at all temperatures. To the best of our knowledge, these $f_{3\text{dB}}$ values for membrane lasers on SiC are all records for DMLs.

Figure 5(a) shows the experimental setup for evaluating the optical eye diagram and bit-error rate (BER) at 25 and 85°C. The 100-Gbit/s NRZ signals with the PRBS of $2^{15}-1$ were generated by an arbitrary waveform generator (AWG) (Keysight M8199A) at 200 GSa/s with an analog $f_{3\text{dB}}$ of 70 GHz. We used a 66-GHz electrical amplifier with a 22-dB gain (SHF M804B) and a 65-GHz electrical amplifier with an 11-dB gain (SHF 827) for the measurements of eye diagrams and BERs, respectively. The DML was driven by a 65-GHz bias tee and a 67-GHz RF probe. Note that, since a pre-emphasis filter was used at AWG to mitigate the RF impairments of the electrical components only for the eye measurements, we were able to evaluate the inherent optical eye diagram reflecting only the laser frequency response. A PDFA was used to amplify the optical power, which was detected with an in-house unitraveling-carrier (UTC) PD

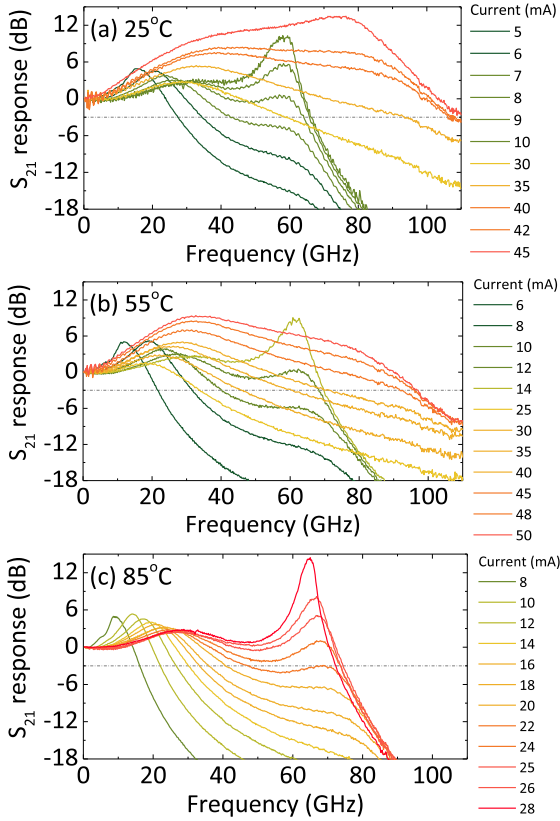


Fig. 4: Small-signal S_{21} responses at (a) 25, (b) 55, and (c) 85°C.

module with a f_{3dB} of >67 GHz. Eye diagrams were acquired using a digital communication analyzer (DCA). For the BER measurements, the received electrical signal with the PD was captured by a real-time digital storage oscilloscope (DSO) with a sampling rate of 160-GSa/s and a bandwidth of ~63 GHz. We used an 11-tap linear equalizer and a 6-tap decision-feedback equalizer to compensate for distortions. Figures 5(b) and (c) show the 100-Gbit/s NRZ optical eye diagrams at 25 and 85°C. The bias currents, bias voltages, and peak-to-peak voltages V_{pp} were 35 mA, 2.97 V, and 1.64 V at 25°C, and 26 mA, 2.43 V, and 1.17 V at 85°C. As shown in Figs. 5 (b) and (c), clear eye openings for 25 and 85°C were obtained with the extinction ratio of 3.3 and 2.9 dB, which verifies the large bandwidth of the DML. Figure 5(d) shows the BER versus received optical power (ROP) for back-to-back (BTB) and 2-km transmissions of 100-Gbit/s NRZ signals. The BERs taken at the current of 35 (27) mA and the V_{pp} of 1.1 V for 25 (85) °C were less than the 5.8%-overhead KP4-FEC threshold of 2.4×10^{-4} . At 25°C, we further evaluated the BER at 8.5 mA in the first PPR-occurrence region, which was less than the 7%-overhead hard-decision forward error correction (HD-FEC) threshold of 3.8×10^{-3} . The lower BERs after the 2-km transmission than the BTB

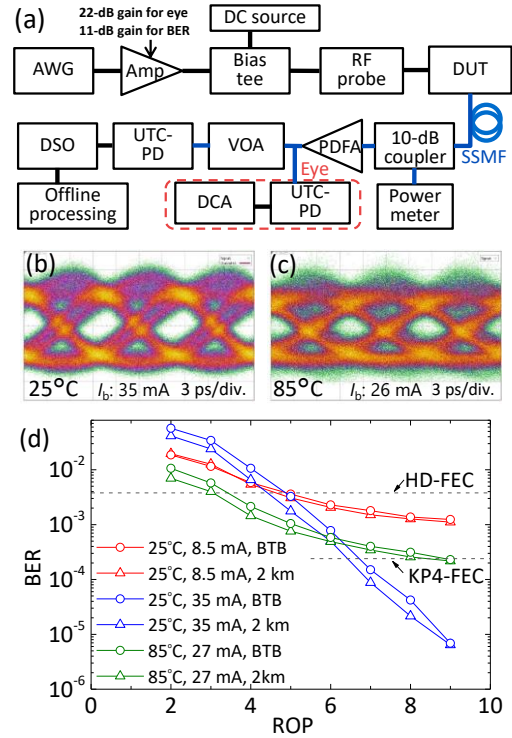


Fig. 5: (a) Experimental setup to measure eye diagram and BER. 100-Gbit/s NRZ eye diagrams at (b) 25°C and (c) 85°C. (d) BER vs. ROP for the 100-Gbit/s NRZ signal transmission.

are presumably due to the negative dispersion of the SSMF [8]. For the first PPR-occurrence region, the energy cost was calculated to be 139 (708) fJ/bit at 25 (85) °C. Note that, at 55°C, the BER taken at 13 (40) mA was less than the HD-(KP4-) FEC thresholds (not shown in the figure).

The fiber-coupled output power was still limited to ~0.8 mW for a 50- μ m-long active region laser at 25°C (the output power directly detected using a PD was ~3 mW) and thus we needed to use PDFFA, whereas the >10-mW output power was expected from the calculation. The ways to increase the fiber-coupled output power include integrating a spot-size converter [9], enlarging the active length, and optimizing the fabrication processes, all of which are currently under investigation.

Conclusions

In this paper, we have investigated the high-temperature-operation characteristics of a membrane laser on a SiC substrate. The device exhibited a large f_r at 85°C thanks to the high thermal conductivity of SiC. By combining the PPR effect, we were able to achieve a maximum f_{3dB} of >110 GHz at 25°C, 97 GHz at 55°C, and 74 GHz at 85°C. We have also demonstrated the 2-km transmission of a 100-Gbit/s NRZ signal at 25 and 85°C. Such DMLs are promising for uncooled 100-Gbaud operation for 800-Gbit/s and 1.6-Tbit/s Ethernet.

References

- [1] 800G Pluggable MSA 2ND WHITE PAPER, "200G PER LANE FOR FUTURE 800G & 1.6T MODULES", <https://www.800gmsa.com/documents/200g-per-lane-for-future-800g-and-16t-modules>
- [2] L. A. Coldren, S. W. Corzine, and M. L. Mashanovitch, *Diode Lasers and Photonic Integrated Circuits*, 2nd ed., Wiley, 2012, Chap. 5, DOI: [10.1002/9781118148167](https://doi.org/10.1002/9781118148167)
- [3] J. Kreissl, V. Vercesi, U. Troppenz, T. Gaertner, W. Wenisch, and M. Schell, "Up to 40 Gb/s Directly Modulated Laser Operating at Low Driving Current: Buried-Heterostructure Passive Feedback Laser (BH-PFL)", *IEEE Photon. Technol. Lett.*, vol. 24, no. 5, pp. 362–364, 2012, DOI: [10.1109/LPT.2011.2179530](https://doi.org/10.1109/LPT.2011.2179530)
- [4] S. Yamaoka, N.-P. Diamantopoulos, H. Nishi, R. Nakao, T. Fujii, K. Takeda, T. Hiraki, T. Tsurugaya, S. Kanazawa, H. Tanobe, T. Kakitsuka, T. Tsuchizawa, F. Koyama, and S. Matsuo, "Directly modulated membrane lasers with 108 GHz bandwidth on a high-thermal-conductivity silicon carbide substrate", *Nat. Photonics*, vol. 15, no. 1, pp. 28–35, 2021, DOI: [10.1038/s41566-020-00700-y](https://doi.org/10.1038/s41566-020-00700-y)
- [5] Y. Matsui, R. Schatz, D. Che, F. Khan, M. Kwakernaak, and T. Sudo, "Low-chirp isolator-free 65-GHz-bandwidth directly modulated lasers", *Nat. Photonics*, vol. 15, no. 1, pp. 59–63, 2021, DOI: [10.1038/s41566-020-00742-2](https://doi.org/10.1038/s41566-020-00742-2)
- [6] N. P. Diamantopoulos, T. Fujii, S. Yamaoka, H. Nishi, K. Takeda, T. Tsuchizawa, T. Segawa, T. Kakitsuka, and S. Matsuo, "60 GHz Bandwidth Directly Modulated Membrane III-V Lasers on SiO₂/Si", *J. Light. Technol.*, pp. 1–9, 2022, DOI: [10.1109/JLT.2022.3153648](https://doi.org/10.1109/JLT.2022.3153648)
- [7] K. Nakahara, K. Suga, K. Okamoto, S. Hayakawa, M. Arasawa, T. Nishida, R. Washino, T. Kitatani, M. Mitaki, H. Sakamoto, Y. Sakuma, and S. Tanaka, "112-Gb/s PAM-4 Uncooled Directly Modulated BH Lasers", *2021 European Conference on Optical Communication (ECOC)*, Bordeaux, France, 2021, pp. 1-3, DOI: [10.1109/ECOC52684.2021.9606099](https://doi.org/10.1109/ECOC52684.2021.9606099)
- [8] N.-P. Diamantopoulos, W. Kobayashi, H. Nishi, K. Takeda, T. Kakitsuka, and S. Matsuo, "Amplifierless PAM-4/PAM-8 transmissions in O-band using a directly modulated laser for optical data-center interconnects", *Opt. Lett.*, vol. 44, no. 1, pp. 9–12, 2019, DOI: [10.1364/OL.44.000009](https://doi.org/10.1364/OL.44.000009)
- [9] H. Nishi, T. Fujii, K. Takeda, K. Hasebe, T. Kakitsuka, T. Tsuchizawa, T. Yamamoto, K. Yamada, and S. Matsuo, "Membrane distributed-reflector laser integrated with SiO_x-based spot-size converter on Si substrate", *Opt. Express*, vol. 24, no. 16, pp. 18346–18352, 2016, DOI: [10.1364/OE.24.018346](https://doi.org/10.1364/OE.24.018346)